



CHORUS

This is the accepted manuscript made available via CHORUS. The article has been published as:

Quantum Computing with Majorana Kramers Pairs

Constantin Schrade and Liang Fu

Phys. Rev. Lett. **129**, 227002 — Published 23 November 2022

DOI: [10.1103/PhysRevLett.129.227002](https://doi.org/10.1103/PhysRevLett.129.227002)

Quantum Computing with Majorana Kramers Pairs

Constantin Schrade and Liang Fu

Department of Physics, Massachusetts Institute of Technology, 77 Massachusetts Ave., Cambridge, MA 02139

(Dated: October 20, 2022)

We propose a universal gate set acting on a qubit formed by the degenerate ground states of a Coulomb-blockaded time-reversal invariant topological superconductor island with spatially separated Majorana Kramers pairs: the “Majorana Kramers Qubit”. All gate operations are implemented by coupling the Majorana Kramers pairs to conventional superconducting leads. Interestingly, in such an all-superconducting device, the energy gap of the leads provides another layer of protection from quasiparticle poisoning independent of the island charging energy. Moreover, the absence of strong magnetic fields – which typically reduce the superconducting gap size of the island – suggests a unique robustness of our qubit to quasiparticle poisoning due to thermal excitations. Consequently, the Majorana Kramers Qubit should benefit from prolonged coherence times and may provide an alternative route to a Majorana-based quantum computer.

PACS numbers: 03.67.Lx; 74.50.+r; 85.25.Cp; 71.10.Pm

In recent years an increasing number of platforms have been proposed for realizing time-reversal invariant topological superconductors (TRI TSCs) [1]. Among the most notable platforms are nanowires and topological insulators in contact to unconventional superconductors (SCs) [2–5] and conventional SCs [6–11], proximity-induced Josephson π -junctions in nanowires and topological insulators [12–15] as well as TSCs with an emergent time-reversal symmetry (TRS) [16–19].

A common feature of TRI TSCs is that they host spatially separated Majorana Kramers pairs (MKPs) which form robust, zero energy modes protected by TRS. In spite of much fundamental interest in the properties of MKPs [20–26], a yet unsolved question is if MKPs can be employed for applications in quantum computation. Here, we answer this question in the affirmative.

The purpose of this work is to introduce a qubit formed by the degenerate ground states of a Coulomb-blockaded TRI TSC island with spatially separated MKPs: the “Majorana Kramers Qubit” (MKQ). We depict the minimal experimental setup for a single MKQ in Fig. 1. It comprises two SC leads which separately couple to two distinct MKPs on a U-shaped TRI TSC island. The two SC leads are also coupled among themselves by normal and spin-flip tunnelling barriers.

Within this setup, we implement single-qubit Clifford gates not by braiding of MKPs [27, 28] but rather by making use of a measurement-based approach to Majorana quantum computing [29, 30]. In such a measurement-based approach, we perform read-out of Majorana bilinears, which correspond to the Pauli operators of our qubit, through Josephson current measurement. More specifically, we selectively deplete either the normal or the spin-flip tunneling barrier and, in this way, realize Josephson couplings that contain different Majorana bilinears, see Fig. 2. To achieve universal quantum computing, we further propose an unprotected T -gate and entangling gate by pulsing of tunnel couplings.

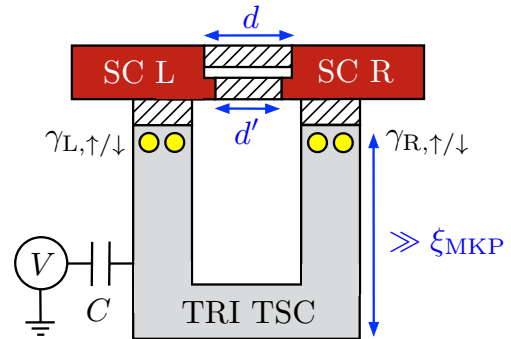


FIG. 1. (Color online) Setup comprised of a U-shaped TRI TSC island (gray) realizing a MKQ. Tunnel couplings (white, dashed) connect the SC leads $\ell = L, R$ (red) to the MKPs $\gamma_{\ell, s}$ (yellow) with $s = \uparrow, \downarrow$. The SC leads are connected by gate-tunable spin-flip and a normal tunnelling barriers with lengths d, d' . To facilitate Cooper pair splitting between these two tunnelling barriers and the TRI TSC island, the separation of the tunnelling contacts is smaller than the coherence length ξ_{SC} of the SC leads. To avoid couplings of the MKPs to fermionic corner modes [31], the length of the vertical TRI TSC segments is much longer than the MKP localization length ξ_{MKP} . A gate voltage V tunes the charge on the TRI TSC island via a capacitor with capacitance C .

The main conceptual lesson we learn is that Majorana-based quantum computing is possible without the need for magnetic fields. In particular, this point differentiates our proposal from previous works [32–41] that propose quantum computing architectures based on conventional Majorana bound states, which in the available experimental candidate platforms require the use of strong magnetic fields for their realization. In particular, the absence of such strong magnetic fields in our proposal constitutes a fundamental advantage because magnetic fields act detrimentally on superconductors and, as a result, constitute a significant challenge towards realizing topological superconductivity. Besides that, there are two features of our setup that yield improved protection

from quasiparticle poisoning: (1) Within the single-MKQ setup of Fig. 1, single-electron tunnelling from the SC leads does not only require overcoming the charging energy of the TRI TSC island but also the breaking of a Cooper pair in the leads. Consequently, the SC gap of the leads provides an additional layer of protection against quasiparticle poisoning, independent of the island charging energy. (2) Quasiparticle poisoning due to thermal excitations within the TRI TSC island is suppressed the SC gap of the island itself. In particular, the energy gap of a TRI TSC may be larger than the energy gap of TRS-breaking Majorana island [32–43] since there is no magnetic field reducing the SC gap size. However, despite the absence of magnetic fields, repulsive interactions, which are present in certain TRI TSC setups [7, 13], could suppress the SC gap size.

Setup. As shown in Fig. 1, our setup comprises a U-shaped TRI TSC islands hosting MKPs $\gamma_{\ell,s}$ with $s = \uparrow, \downarrow$ at spatially well separated boundaries $\ell = L, R$. The two members of a MKP are related by TRS,

$$\mathcal{T}\gamma_{\ell,\uparrow}\mathcal{T}^{-1} = \gamma_{\ell,\downarrow}, \quad \mathcal{T}\gamma_{\ell,\downarrow}\mathcal{T}^{-1} = -\gamma_{\ell,\uparrow}. \quad (1)$$

We assume that the dimensions of the vertical island segments exceed the MKP localization length, ξ_{MKP} , to avoid couplings to fermionic modes that are potentially localized at the island corners [31]. The MKPs are then robust zero-energy states protected by TRS.

Since the TRI TSC island is of mesoscopic size, it acquires (like mesoscopic TSC islands with broken time-reversal symmetry [42]) a charging energy given by

$$U_C = (ne - Q)^2 / 2C. \quad (2)$$

Here, Q is the island gate charges that is continuously tunable with a voltage across a capacitor with capacitance C . We tune the gate charge Q/e so that the ground state of the TRI TSC island comprises n_0 electron charges. For a sufficiently large charging energy $e^2/2C$, the joint parity of the MKPs on the TRI TSC island is then given by [42, 44]

$$\gamma_{L,\uparrow}\gamma_{R,\uparrow}\gamma_{L,\downarrow}\gamma_{R,\downarrow} = (-1)^{n_0}. \quad (3)$$

We note that this parity constraint applies to the MKPs on the *same* TRI TSC, which is different from quantum computing proposals based on conventional Majorana bound states that require two *different* TSCs that are connected by a conventional SC bridge [39–41]. The parity constraint reduces the four-fold degeneracy of the ground state at zero charging energy, to a two-fold degenerate ground state which forms the MKQ. The Pauli operators acting on each of the two MKQs can be written as bilinears in the Majorana operators,

$$\hat{x} = i\gamma_{R,\uparrow}\gamma_{L,\downarrow}, \quad \hat{y} = i\gamma_{R,\uparrow}\gamma_{R,\downarrow}, \quad \hat{z} = i\gamma_{R,\downarrow}\gamma_{L,\downarrow}. \quad (4)$$

Under TRS, the Pauli operators transform as $\mathcal{T}\hat{x}\mathcal{T}^{-1} = (-1)^{n_0}\hat{x}$, $\mathcal{T}\hat{y}\mathcal{T}^{-1} = -\hat{y}$ and $\mathcal{T}\hat{z}\mathcal{T}^{-1} = (-1)^{n_0}\hat{z}$. We note

again that the Pauli operators are defined in terms of MKPs on the same TRI TSC islands, unlike the Pauli operators in quantum computing proposals based on Majorana bound states that are localized on different TSCs connected by a conventional SC bridge [39–41].

In our setup, we choose to address the MKQ by weakly coupling each MKP to a separate s -wave SC lead. The Hamiltonian for the two SC leads is of the standard BCS (BardeenCooperSchrieffer) form,

$$H_{SC} = \sum_{\ell=L,R} \sum_{\mathbf{k}} \Psi_{\ell,\mathbf{k}}^\dagger (\xi_{\mathbf{k}}\eta_z + \Delta_\ell\eta_x e^{i\varphi_\ell\eta_z}) \Psi_{\ell,\mathbf{k}}, \quad (5)$$

where $\Psi_{\ell,\mathbf{k}} = (c_{\ell,\mathbf{k}\uparrow}, c_{\ell,-\mathbf{k}\downarrow}^\dagger)^T$ is a Nambu spinor with $c_{\ell,\mathbf{k}s}$ the electron annihilation operator at momentum \mathbf{k} and spin s in lead ℓ . The Pauli matrices $\eta_{x,y,z}$ act in Nambu-space. Furthermore, $\xi_{\mathbf{k}}$ is the normal state dispersion and $\Delta_\ell, \varphi_\ell$ denote magnitude and phase of the SC order parameter of the m -SC lead. The SC phase difference is $\varphi \equiv \varphi_L - \varphi_R$. We assume low temperatures, so no quasiparticle states in the SC leads are occupied with notable probability and can couple to the MKPs.

The most general tunneling Hamiltonian between the MKPs and the fermions on the ℓ -SC lead reads,

$$H_T = \sum_{\ell=L,R} \sum_{\mathbf{k},s} \lambda_\ell c_{\ell,\mathbf{k}s}^\dagger \gamma_{\ell,s} e^{-i\phi/2} + \text{H.c.}, \quad (6)$$

where we have diagonalized the tunnelling Hamiltonian in spin-space by an appropriate rotation of the lead fermions [26]. This rotation constraints the point-like tunnelling amplitudes λ_ℓ to be real numbers, a consequence of the time-reversal symmetry that is not present in quantum computing proposals based on conventional Majorana bound states [41]. The operators $e^{\pm i\phi/2}$ raise/lower the total island charges by one unit, $[n, e^{\pm i\phi/2}] = \pm e^{\pm i\phi/2}$, while the MBSs operators $\gamma_{\ell,s}$ flip the respective electron number parities.

As evident from Fig. 1, there are two types of couplings between the SC leads: The first type is an *indirect coupling* via the TRI TSC islands which is induced by the tunnelling Hamiltonian of Eq. (6). The second type is a *direct coupling* via two additional tunnelling barriers. The first tunnelling barrier is used for measuring the \hat{z} -Pauli operator and only allows for normal tunnelling,

$$H_N = t_N \sum_{\mathbf{k}} c_{R,\mathbf{k}\uparrow}^\dagger c_{L,\mathbf{k}\uparrow} + c_{L,\mathbf{k}\downarrow}^\dagger c_{R,\mathbf{k}\downarrow} + \text{H.c.}, \quad (7)$$

where t_N is a complex, point-like tunnelling amplitude. The second barrier is used for measuring the \hat{x} -Pauli operator and only permits spin-flip tunnelling,

$$H_S = t_S \sum_{\mathbf{k}} c_{R,\mathbf{k}\uparrow}^\dagger c_{L,\mathbf{k}\downarrow} - c_{L,\mathbf{k}\uparrow}^\dagger c_{R,\mathbf{k}\downarrow} + \text{H.c.}, \quad (8)$$

where t_S is again a complex, point-like tunnelling amplitude. For the \hat{x} (\hat{z}) measurement protocols, we require

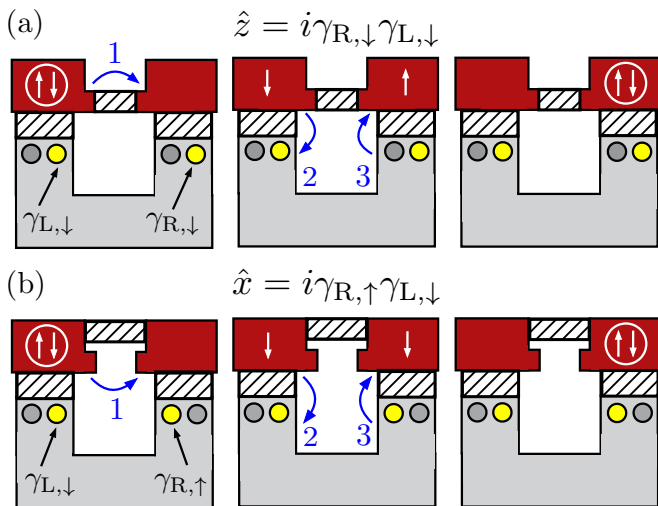


FIG. 2. (Color online) (a) A sequence of intermediate states in which a Cooper pair moves between the SC leads by splitting up between the normal tunnelling barrier and the TRI TSC. The spin-flip tunnelling barrier is fully depleted. The MBS operators (not) participating in the sequence are shown in yellow (gray). The resulting effective coupling is $\propto \hat{z}$. (b) Same as (a) but now the Cooper pair splits up between the spin-flip tunnelling barrier and the TRI TSC. The normal tunnelling barrier is fully depleted. The coupling is $\propto \hat{x}$.

$\text{Im } t_S \neq 0$ ($\text{Im } t_N \neq 0$) when n_0 even and $\text{Re } t_S \neq 0$ ($\text{Re } t_N \neq 0$) when n_0 odd. In addition, we propose two ways to engineer such tunnelling barriers: (1) We consider barriers with a finite *intrinsic* spin-orbit coupling with spin-orbit length λ_{SO} as well as different barrier lengths d, d' . Tuning λ_{SO}/d' (λ_{SO}/d) to a positive integer (positive half integer) realizes a barrier with pure normal (spin-flip) tunnelling [45]. (2) We consider barriers with an *engineered* spin-orbit coupling due to a local, rotating magnetic field induced by a series of nanomagnets [46, 47]. By adjusting the the rotating field period through the nanomagnet separation, we can realize barriers with pure normal or spin-flip tunnelling.

In summary, the full Hamiltonian reads $H = U_C + H_{\text{SC}} + H_T + H_N + H_S$.

Single-qubit Clifford gates. In this section, we will implement single-qubit Clifford gates by “Majorana tracking” [30]. This means for a given circuit of single-qubit Clifford gates we record all Pauli operator redefinitions on a classical computer and use the quantum hardware only to perform suitable measurements of the $\hat{x}, \hat{y}, \hat{z}$ -Pauli operators at the end of the computation.

First, for measuring the \hat{z} -Pauli operator, we consider the situation when a local gate depletes the spin-flip tunnelling barrier between the two SC leads, $\text{Im } t_S = 0$ for n_0 even and $\text{Re } t_S = 0$ for n_0 odd.

In this case, to second order in t_N , Cooper pairs tunnel between the SC leads only via the normal tunnelling barrier inducing a finite Josephson coupling $J_N \sim 2|t_N|^2/\Delta$.

In particular, a Josephson coupling due to Cooper tunnelling between each SC lead and the TRI TSC is unfavorable due to the substantial island charging energy [41]. The island charging energy thus plays two key roles: First, it suppresses quasiparticle poisoning due to single-electron tunnelling from the environment. Second, it suppresses local mixing $\propto \hat{y}$ due to Cooper pair tunnelling between each SC lead and the TRI TSC island. Such local mixing terms are – as noticed earlier [49] – of importance for TRI TSCs with zero charging energy and, as we will see, can be used to measure the \hat{y} -Pauli operator.

Next, we note that to third order in $t_N, \lambda_L, \lambda_R$ Cooper pair splitting sequences between the TRI TSC island and the normal tunnelling barrier induce additional Josephson couplings, J_z for n_0 even and J'_z for n_0 odd, see Fig. 2(a). In a first process, a Cooper pair on the left SC lead breaks up and one of the electrons tunnels via the normal tunnelling barrier to the right SC lead. This leaves the left SC lead in an excited state with one quasiparticle above the SC gap. In a second process, the quasiparticle on the left SC tunnels to the TRI TSC island and increments its charge by one unit. While the left SC returns to its ground state in this way, the TRI TSC island is now in an excited state with one excess charge. It, therefore, requires a third process to remove the extra charge from the TRI TSC by recombining it to a Cooper pair on the right SC lead. Critically, the tunnelling events via both the normal tunnelling barrier and the TRI TSC island conserve the electron spin. For that reason, the just described third-order sequences contribute terms $\propto \hat{z} = i\gamma_{R,\downarrow}\gamma_{L,\downarrow} = (-1)^{n_0}i\gamma_{L,\uparrow}\gamma_{R,\uparrow}$.

For $\pi\nu_\ell\lambda_\ell^2 \ll \Delta, e^2/2C$ with ν_ℓ the normal-state density of states per spin of the ℓ -SC lead at the Fermi energy, we compute the amplitudes of all above-mentioned sequences perturbatively. Up to third order in the tunnelling amplitudes, we obtain an effective Hamiltonians acting on the ground states of the SC leads and the TRI TSC island. For n_0 even and n_0 odd, we find,

$$\begin{aligned} H_{z,\text{even}} &= -(J_N + \hat{z} J_z) \cos \varphi, \\ H_{z,\text{odd}} &= -J_N \cos \varphi + \hat{z} J'_z \sin \varphi. \end{aligned} \quad (9)$$

The Josephson couplings are $J_z = \text{Im}(t_N)\lambda^2\nu_F\alpha/\Delta$ and $J'_z = -\text{Re}(t_N)\lambda^2\nu_F\alpha/\Delta$, where we assumed $\lambda_L = \lambda_R \equiv \lambda$, $\nu_L = \nu_R \equiv \nu_F$, and α is a dimensionless prefactor of order one if $U \sim \Delta$ [48]. Notably, J_z [J'_z] and J are of comparable magnitude if we choose the coupling between the SC leads so that $\nu_F\lambda^2 \gtrsim 2|t_N|^2/(\text{Im}(t_N)\alpha)$ [$\nu_F\lambda^2 \gtrsim 2|t_N|^2/(\text{Re}(t_N)\alpha)$]. Also, we note that both effective Hamiltonians exhibit TRS: For $H_{z,\text{even}}$ both \hat{z} and $\cos \varphi$ are time-reversal even, while for $H_{z,\text{odd}}$ both \hat{z} and $\sin \varphi$ are time-reversal odd.

To measure the z -eigenvalue of the \hat{z} -Pauli operator, we adopt a two-step protocol: (1) First, we separately measure the Josephson current through the normal tunnelling barrier and through the TRI TSC island

to determine J_N and J . (2) Second, we measure the Josephson current through the entire device. For n_0 even, the latter is given by $I = I_c \sin \varphi$ with the critical current $I_c = 2e(J_N + zJ_z)/\hbar$ fixing the z -eigenvalue. For n_0 odd, the current phase relation is of the form $I = I_c \sin(\varphi + \varphi_0)$. This time it is not the critical current $I_c = 2e \operatorname{sgn}(J_N) \sqrt{(J_N)^2 + (J_z)^2}/\hbar$ but the anomalous phase shift $\varphi_0 = z \arctan[J'_z/J_N]$ which fixes the z -eigenvalue. We note that the anomalous phase shift results from the \hat{z} -eigenstates breaking TRS when n_0 odd.

To measure the \hat{x} -Pauli operator, we consider a depleted normal tunnelling barrier, $\operatorname{Im} t_N = 0$ for n_0 even and $\operatorname{Re} t_N = 0$ for n_0 odd. As before, second order co-tunnelling events now induce a Josephson coupling $J_S \sim 2|t_S|^2/\Delta$ as a result of Cooper pair tunnelling via the spin-flip tunnelling barrier whereas fourth order events mediate a Josephson coupling J via the TRI TSC island. However, a qualitative difference to the preceding considerations arises for the third order Cooper pair splitting sequences, see Fig. 2(b). These sequences now demand two spin-flips, one for an electron to move through the spin-flip tunnelling barrier and one for an electron to move through the TRI TSC island. Consequently, the third-order sequences now contribute terms $\propto \hat{x} = i\gamma_{R,\uparrow}\gamma_{L,\downarrow} = (-1)^{n_0}i\gamma_{R,\downarrow}\gamma_{L,\uparrow}$. Up to third order in the tunnel couplings, the effective Hamiltonians for n_0 even and n_0 odd read,

$$\begin{aligned} H_{x,\text{even}} &= -(J_S + \hat{x} J_x) \cos \varphi, \\ H_{x,\text{odd}} &= -J_S \cos \varphi + \hat{x} J'_x \sin \varphi. \end{aligned} \quad (10)$$

Here, $J_x = \operatorname{Im}(t_S)\lambda^2\nu_F\alpha/\Delta$ and $J'_x = -\operatorname{Re}(t_S)\lambda^2\nu_F\alpha/\Delta$, where we assumed $\lambda_L = \lambda_R \equiv \lambda$ and $\nu_L = \nu_R \equiv \nu_F$. We further note that both effective Hamiltonian exhibit TRS: For $H_{x,\text{even}}$ both \hat{x} and $\cos \varphi$ are time-reversal even, while for $H_{x,\text{odd}}$ both \hat{x} and $\sin \varphi$ are time-reversal odd. To measure the \hat{x} -Pauli operator, we see that the effective Hamiltonians are of the same form as those in Eq. (9). Hence, our measurement protocol for the \hat{z} -Pauli operator carries over to \hat{x} -Pauli operator measurements.

We highlight that potential errors in the \hat{x} , \hat{z} -measurements occur when both $\operatorname{Im} t_N \neq 0$, $\operatorname{Im} t_S \neq 0$ for n_0 even or $\operatorname{Re} t_N \neq 0$, $\operatorname{Re} t_S \neq 0$ for n_0 odd. This can happen either if one of the tunnelling barriers is not fully depleted, or the barrier lengths d, d' are not appropriately adjusted to the spin-orbit length λ_{SO} . Fortunately, this constitutes a hardware error addressable prior to experiments. In particular, the error can be made small with a careful design of a *conventional* Josephson junction.

Finally, we address \hat{y} -measurements. These require the tuning the charging energy of the TRI TSC to zero which is attainable – on demand – by coupling the TRI TSC island to a bulk SC through a gate-tunable valve [37]. Critically, even at zero charging energy the value of the joint fermion parity in Eq. (3) remains protected as a result of the lead SC gap. However, unlike in the case

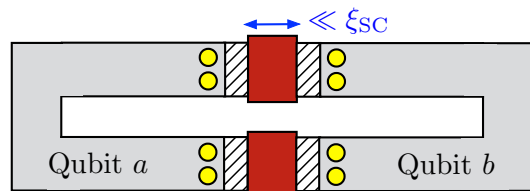


FIG. 3. (Color online) Setup of two MKQs a, b coupled to two SC leads. The width of the leads is much smaller than their SC coherence length ξ_{SC} , thereby, permitting Cooper pair splitting between the two MKQs. The resulting Heisenberg interaction between the MKQs is used for an entangling gate.

of a substantial charging energy, Cooper pairs can now tunnel in a second order process between each SC lead and the TRI TSC island inducing a Josephson coupling $\propto \hat{y}$ [20]. Consequently, the resulting Josephson current provides a means for measuring the \hat{y} eigenvalue. The details of this measurement scheme are discussed in [20].

Universal quantum computation. For universal quantum computation, the single-qubit Clifford gates need to be supplemented by a $T = \exp(-i\hat{z}\pi/8)$ gate and an entangling gate [50]. If n_0 odd [even], we obtain the T -gate by pulsing $J_z \cos(\varphi)$ [$J'_z \cos(\varphi)$] in $H_{z,\text{even}}$ [$H_{z,\text{odd}}$] for a duration τ so that $\int_0^\tau J_z(t') \cos(\varphi(t')) dt' = \pi/8$ [$\int_0^\tau J'_z(t') \cos(\varphi(t')) dt' = \pi/8$]. Due to imprecisions in the pulsing intervals, these operations are not protected. The need for unprotected gates is generic for Majorana qubits [38–41]. Moreover, for the presented procedure, phase-independent contributions – which were irrelevant for the Josephson current – should now be included in the effective Hamiltonians, see [48].

For an entangling gate, we consider the setup of Fig. 3 which comprises two SC leads addressing two MKQs a, b . A local gate depletes both normal and spin-flip tunnelling barrier, $t_N = t_S = 0$. If the width of the SC leads is much smaller than the SC coherence length ξ_{SC} , a Cooper pair can split between the two TRI TSC islands and entangle the MKQs. For symmetric couplings and a ground state charge n_0 for both islands, we have computed the process amplitudes in the weak coupling limit. An anisotropic Heisenberg coupling results,

$$\begin{aligned} H_{ab} &= J_y \hat{y}_a \hat{y}_b \\ &+ [J_{xz} + (-1)^{n_0+1} J'_{xz} \cos \varphi] (\hat{x}_a \hat{x}_b + \hat{z}_a \hat{z}_b). \end{aligned} \quad (11)$$

For the microscopic form of J_{xz}, J'_{xz}, J_y , see [48]. The Heisenberg interaction can be made isotropic by choosing the SC phase difference such that $\tilde{J} \equiv J_y = J_{xz} + (-1)^{n_0+1} J'_{xz} \cos \varphi$. Pulsing the couplings for a time τ defined by $\int_0^\tau \tilde{J}(t') dt' = \pi/2$ then implements a $\sqrt{\text{SWAP}}$ -gate via the unitary time evolution operator. The latter, combined with single-qubit gates, allows for universal quantum computing [51].

Conclusions. We introduced the “Majorana Kramers Qubit” formed by the ground states of a TRI TSC. By

coupling a MKQ to SC leads, single-qubit Clifford gates are realized by qubit measurements. A T -gate and an entangling gate are realized by pulsing Josephson couplings. The MKQ shows that strong magnetic fields are not needed for Majorana-based quantum computing.

Acknowledgments. We would like to thank Jagadeesh S. Moodera for helpful discussions. C.S. was supported by the Swiss SNF under Project 174980. L.F. and C.S. were supported by DOE Office of Basic Energy Sciences, Division of Materials Sciences and Engineering under Award DE-SC0010526.

-
- [1] A. P. Schnyder, S. Ryu, A. Furusaki, and A. W. W. Ludwig, Phys. Rev. B **78**, 195125 (2008).
- [2] C. L. M. Wong and K. T. Law, Phys. Rev. B **86**, 184516 (2012).
- [3] S. Nakosai, J. C. Budich, Y. Tanaka, B. Trauzettel, and N. Nagaosa, Phys. Rev. Lett. **110**, 117002 (2013).
- [4] F. Zhang, C. L. Kane, and E. J. Mele, Phys. Rev. Lett. **111**, 056402 (2013).
- [5] E. Dumitrescu, J. D. Sau, and S. Tewari, Phys. Rev. B **90**, 245438 (2014).
- [6] J. Klinovaja and D. Loss, Phys. Rev. B **90**, 045118 (2014).
- [7] E. Gaidamauskas, J. Paaske, and K. Flensberg, Phys. Rev. Lett. **112**, 126402 (2014).
- [8] C. Schrade, M. Thakurathi, C. Reeg, S. Hoffman, J. Klinovaja, and D. Loss, Phys. Rev. B **96**, 035306 (2017).
- [9] J. Klinovaja, A. Yacoby, and D. Loss, Phys. Rev. B **90**, 155447 (2014).
- [10] Z. Yan, F. Song, and Z. Wang, Phys. Rev. Lett. **121**, 096803 (2018).
- [11] C.-H. Hsu, P. Stano, J. Klinovaja, and D. Loss, Phys. Rev. Lett. **121**, 196801 (2018).
- [12] A. Keselman, L. Fu, A. Stern, and E. Berg, Phys. Rev. Lett. **111**, 116402 (2013).
- [13] A. Haim, A. Keselman, E. Berg, and Y. Oreg, Phys. Rev. B **89**, 220504(R) (2014).
- [14] C. Schrade, A. A. Zyuzin, J. Klinovaja, and D. Loss, Phys. Rev. Lett. **115**, 237001 (2015).
- [15] U. Borla, D. Kuzmanovski, and A. M. Black-Schaffer, Phys. Rev. B **97**, 014507 (2018).
- [16] Y. Huang, C.-K. Chiu, arXiv:1708.05724.
- [17] C. Reeg, C. Schrade, J. Klinovaja, and D. Loss, Phys. Rev. B **96**, 161407(R) (2017).
- [18] H. Hu, F. Zhang, and C. Zhang, Phys. Rev. Lett. **121**, 185302 (2018).
- [19] M. Maisberger, L.-C. Wang, K. Sun, Y. Xu, and C. Zhang, arXiv:1710.08323.
- [20] S. B. Chung, J. Horowitz, X.-L. Qi, Phys. Rev. B **88**, 214514 (2013).
- [21] J. Li, W. Pan, B. A. Bernevig, and R. M. Lutchyn, Phys. Rev. Lett. **117**, 046804 (2016).
- [22] D. I. Pikulin, Y. Komijani, and I. Affleck, Phys. Rev. B **93**, 205430 (2016).
- [23] Y. Kim, D. E. Liu, E. Gaidamauskas, J. Paaske, K. Flensberg, and R. M. Lutchyn, Phys. Rev. B **94**, 075439 (2016).
- [24] A. Camjayi, L. Arrachea, A. Aligia, and F. von Oppen, Phys. Rev. Lett. **119**, 046801 (2017).
- [25] Z. Q. Bao, F. Zhang, Phys. Rev. Lett. **119**, 187701 (2017).
- [26] C. Schrade and L. Fu, Phys. Rev. Lett. **120**, 267002 (2018).
- [27] X.-J. Liu, C. L.M. Wong, and K.T. Law, Phys. Rev. X **4**, 021018 (2014).
- [28] P. Gao, Y.-P. He, and X.-J. Liu, Phys. Rev. B **94**, 224509 (2016).
- [29] P. Bonderson, M. Freedman, and C. Nayak, Phys. Rev. Lett. **101**, 010501 (2008).
- [30] D. Litinski and F. von Oppen, Phys. Rev. B **96**, 205413 (2017).
- [31] J. Klinovaja and D. Loss, Eur. Phys. J. B **88**, 62 (2015).
- [32] S. Vijay, T. H. Hsieh, and L. Fu, Phys. Rev. X **5**, 041038 (2015).
- [33] S. Vijay and L. Fu, Phys. Scr. **2016** 014002.
- [34] L. A. Landau, S. Plugge, E. Sela, A. Altland, S. M. Albrecht, and R. Egger, Phys. Rev. Lett. **116**, 050501 (2016).
- [35] S. Plugge, L. A. Landau, E. Sela, A. Altland, K. Flensberg, and R. Egger, Phys. Rev. B **94**, 174514 (2016).
- [36] S. Vijay and L. Fu, Phys. Rev. B **94**, 235446 (2016).
- [37] D. Aasen, M. Hell, R. V. Mishmash, A. Higginbotham, J. Danon, M. Leijnse, T. S. Jespersen, J. A. Folk, C. M. Marcus, K. Flensberg, and J. Alicea, Phys. Rev. X **6**, 031016 (2016).
- [38] S. Hoffman, C. Schrade, J. Klinovaja, and D. Loss, Phys. Rev. B **94**, 045316 (2016).
- [39] T. Karzig, C. Knapp, R. M. Lutchyn, P. Bonderson, M. B. Hastings, C. Nayak, J. Alicea, K. Flensberg, S. Plugge, Y. Oreg, C. M. Marcus, and M. H. Freedman, Phys. Rev. B **95**, 235305 (2017).
- [40] S. Plugge, A. Rasmussen, R. Egger, and K. Flensberg, New J. Phys **19**, 012001 (2017).
- [41] C. Schrade and L. Fu, Phys. Rev. Lett. **121**, 267002 (2018).
- [42] L. Fu, Phys. Rev. Lett. **104**, 056402 (2010).
- [43] M. Gau, S. Plugge, and R. Egger, Phys. Rev. B **97**, 184506 (2018).
- [44] C. Xu and L. Fu, Phys. Rev. B, **81**.134435 (2010).
- [45] D. Bercioux and P. Lucignano, Report on Progress in Physics **78**, 106001 (2015).
- [46] B. Karmakar, D. Venturelli, L. Chirolli, F. Taddei, V. Giovannetti, R. Fazio, S. Roddaro, G. Biasiol, L. Sorba, V. Pellegrini, and F. Beltram, Phys. Rev. Lett. **107**, 236804 (2011).
- [47] J. Klinovaja and D. Loss, Phys. Rev. X **3**, 011008 (2013).
- [48] In the Supplemental Material, we provide more details on the derivation of the effective Hamiltonians required for the implementation of the single- and two-qubit quantum gates.
- [49] K. Wölms, A. Stern, and K. Flensberg, Phys. Rev. Lett. **113**, 246401 (2014).
- [50] J.-L. Brylinski and R. Brylinski, arXiv:quant-ph/0108062.
- [51] D. Loss and D. P. DiVincenzo, Phys. Rev. A **57**, 120 (1998).